Transition Met Chem (2013) 38:299–305
DOI 10.1007/s11243-013-9691-y

Two palladium(II) complexes based on Schiff base ligands: synthesis, characterization, luminescence, and catalytic activity

**Hai-Fu Guo · Xin Zhao · De-Yun Ma ·
Ai-Ping Xie · Wei-Bo Shen**

Received: 20 December 2012 / Accepted: 4 January 2013 / Published online: 19 January 2013

Abstract Two Pd(II) complexes involving Schiff base ligands, namely, $[Pd(L1)_2]$ (**1**), $[Pd_2(L_2)Cl_2]$ (**2**) [**HL1** = 2-((2,6-diisopropylphenylimino)methyl)-4,6-dibromophenol, **L2** = *N*-(4-isopropylbenzylidene)-2,6-diisopropylbenzenamine] have been synthesized using solvothermal methods and characterized by elemental analysis, IR-spectroscopy, thermogravimetric analysis, powder X-ray diffraction, UV–vis absorption spectra, and single-crystal X-ray diffraction. Complex **1** is a mononuclear cyclometalated Pd(II) complex, whereas complex **2** is a μ-chloro-bridged dinuclear. Both **1** and **2** display photoluminescence in the solid state at 298 K and possess fluorescence lifetimes ($\tau_1 = 86.40$ ns, $\tau_2 = 196.21$ ns, $\tau_3 = 1{,}923.31$ ns at 768 nm for **1**, $\tau_1 = 69.92$ ns, $\tau_2 = 136.40$ ns, $\tau_3 = 1{,}714.26$ ns at 570 nm for **2**). The Suzuki reactions of 4-bromotoluene with phenylboronic acid by complexes **1**–**2** have also been studied.

Introduction

Schiff bases continue to be of considerable interest as ligands that are used in conjunction with palladium metals. This class of compounds displays diverse structural features and in some instances exhibits interesting reactivities and photoluminescence [1–6]. However, compared with platinum(II) complexes involving Schiff base ligands, whose applications as luminescent sensors are of considerable interest in inorganic photochemistry [7, 8], relatively scant attention has been focused upon the luminescent characteristics of palladium(II) complexes [2]. In general, luminescent cyclopaladated complexes show low efficiency emissions detected only at low temperatures [9] due to the presence of thermally accessible low-lying metal centered states (MC) that allow excited states to experience non-radiative decay [10]. Moreover, the palladium-catalyzed formation of biaryls from arylhalides with arylboronic acids (the Suzuki reaction) has become one of the mainstays of modern synthetic organic chemistry for the formation of carbon–carbon bonds [11, 12]. Compared with homogeneous catalysis for such coupling reactions, heterogeneous catalysis involving supported metal complexes offers several advantages, such as robustness and increased air and moisture stability [13, 14]. Various supports, including silica, sepiolites, zeolites and polymers, have been used to heterogenize the homogeneous catalysts [15–18]. Palladium(II) complexes derived from Schiff base ligands have been extensively studied over the past few decades in the light of their applications as heterogeneous catalysts in organic reactions [19]. As part of our ongoing investigation into the palladium complexes involving Schiff base ligands [19], we here report the synthesis, characterization, luminescent properties, and catalytic activities of two new Pd(II) complexes based on Schiff base ligands.

Experimental

All chemicals were commercially available and used as received without further purification. Elemental analyses for C, H, and N were carried out using a Vario EL III Elemental

---

Electronic supplementary material The online version of this article (doi:10.1007/s11243-013-9691-y) contains supplementary material, which is available to authorized users.

H.-F. Guo (✉) · X. Zhao · D.-Y. Ma · A.-P. Xie · W.-B. Shen
School of Chemistry and Chemical Engineering, Zhaoqing University, Zhaoqing 526061, People's Republic of China
e-mail: guohaifu@zqu.edu.cn

X. Zhao
College of Chemical Engineering, Inner Mongolia University of Technology, Inner Mongolia 010051, People's Republic of China

Analyzer. Infrared spectra were recorded (4,000–400 cm^{-1}) as KBr disks on a Shimadzu IR-440 spectrometer. Thermogravimetric analyses (TGA) were performed on an automatic simultaneous thermal analyzer (DTG-60, Shimadzu) under a flow of N_2 at a heating rate of 10 °C/min between ambient temperature and 800 °C. Powder XRD investigations were carried out on a Bruker AXS D8-Advanced diffractometer at 40 kV and 40 mA with Cu-Kα ($\lambda = 1.5406$ Å) radiation. UV–vis absorption spectra were measured using a Shimadzu UV-160A spectrophotometer. Luminescence spectra and lifetimes for crystalline samples were recorded at room temperature on an Edinburgh FLS920 phosphorimeter. Nuclear magnetic resonance spectra were recorded on a Bruker Avance 400 MHz spectrometer. ^{1}H-NMR chemical shifts are reported in ppm from tetramethylsilane with the solvent resonance as the internal standard ($CDCl_3$, $\delta = 7.26$). Data are reported as follows: chemical shift (δ ppm), multiplicity (s = singlet, d = doublet, t = triplet, m = multiplet), coupling constants (Hz), integration, and assignment. ^{13}C-NMR spectra were collected on a 100 MHz spectrometer with complete proton decoupling. Chemical shifts are reported in ppm from the tetramethylsilane (TMS) with the solvent resonance as internal standard ($CDCl_3$, $\delta = 77.23$). Melting points were measured uncorrected with a Mel-Temp apparatus.

Preparation of **HL1**

The preparation of **HL1** was carried out according to the reported procedures [20].Yield 4.75 g (52 %). IR (KBr, cm^{-1}): 3,473(s), 2,962(s), 2,883(w), 1,622(vs), 1,444(s), 1,382(w), 1,352 (m), 1,323(w), 1,290(m), 1,217(w), 1,161(s), 1,101(w), 1,056(w), 991(w), 945(w), 867(w), 804(m), 759(m), 717(m), 684(s), 570(w), 505(w).

Preparation of L2 (**L2**)

L2 was prepared by the condensation of cuminaldehyde (2.96 g, 20 mmol) with 2,6-diisopropylaniline (3.55 g, 20 mmol) in ethanol (20 mL) as the reaction medium. The solution was refluxed for 4 h and then allowed to cool at room temperature. The yellow precipitate was recrystallized from ethanol to give **L2** as straw yellow crystals. Yield 4.29 g (66 %). ^{1}H NMR (400 MHz, $CDCl_3$) δ: 8.16 (s, 1H, C**H**N), 7.09–7.85 (m, 6H, Ar–H), 2.98 [t, $J = 4.56$ Hz, 3H, C**H**$(CH_3)_2$], 1.23 (q, $J = 4.68$ Hz, 18H, CH_3); ^{13}C NMR (100 MHz, $CDCl_3$) δ: 161.8, 152.8, 149.4, 137.7, 133.9, 128.7, 126.9, 124.0, 123.0, 77.2, 77.0, 76.8, 34.3, 27.9, 23.9, 23.5. Anal. Calcd for $C_{22}H_{28}N$: C, 86.27; H, 9.15; N, 4.58. Found: C, 86.32; H, 9.12; N, 4.56. IR (KBr, cm^{-1}): 3,456(s), 2,966(s), 2,871(m), 1,641(vs), 1,606(m), 1,573(w), 1,508(m), 1,461(m), 1,438(w), 1,380(w), 1,363(m), 1,325(w), 1,307(s), 1,255(w), 1,240(w), 1,176(s), 1,097(s), 1,054(s), 1,018(w), 993(w), 931(m), 873(m), 837(s), 796(m), 759(s), 731(m), 667(w), 599(w), 557(m), 459(w). MP: 84–85 °C.

Preparation of $[Pd(L1)_2]$ (**1**)

Na_2PdCl_4 (0.0887 g, 0.5 mmol) was dissolved in methanol (10 mL). **HL1** (0.426 g, 1 mmol) was added and the mixture stirred at room temperature for 5 h under an anhydrous atmosphere. The resulting mixture was filtered under reduced pressure. The collected solid was washed with ethyl ether and dried in air to give yellow crystals that were purified by recrystallization from methylene chloride (15 mL) and hexane (10 mL). Yield 0.382 g (78 %). Anal. For $C_{38}H_{40}Br_4N_2O_2Pd$ (%): Calcd. C 46.40, H 4.07, N 2.85; Found C: 46.45, H 4.05, N 2.83. FTIR (KBr, cm^{-1}): 3,450(s), 2,962(s), 2,931(w), 2,875(w), 1,608(vs), 1,504(m), 1,433(s), 1,402(w), 1,384(w), 1,311(s), 1,218(w), 1,155(s), 1,101(w), 1,058(w), 945(w), 889(w), 856(w), 806(w), 769(m), 748(w), 723(m), 671(w), 640(w), 538(m).

Preparation of $[Pd_2(L_2)Cl_2]$ (**2**)

Complex **2** was prepared by the same procedure as **1** except that **HL1** was replaced with **L2**. Yield 0.182 g (81 %); Anal for $C_{44}H_{56}Cl_2N_2Pd_2$ (%): Calcd. C 58.89, H 6.25, N 3.12; Found C 58.94, H 6.28; N 3.08. FTIR (KBr, cm^{-1}): 3,467(s), 2,962(s), 2,871(w), 1,597(s), 1,583(vs), 1,456(s), 1,409(w), 1,398(w), 1,380(w), 1,328(m), 1,282(m), 1,226(m), 1,178(m), 1,135(m), 1,056(m), 1,037(w), 983(w), 935(w), 892(w), 819(m), 800(m), 763(m), 757(w), 611(w), 535(w), 420(m).

Catalytic reactions

A mixture of 4-bromotoluene (1.0 mmol), phenylboronic acid (1.2 mmol), organic solvents (6 mL), base (2.0 mmol), and 0.5 mol % of catalyst was stirred at 80 °C under air. After the reaction, the catalyst was separated by filtration. The filtrate was dried over Na_2SO_4 and again filtered. The products were quantified by GC–MS analysis (Shimadzu GCMS-QP5050A equipped with a 0.25 mm × 30 m DB-WAX capillary column). The typical GC–MS analysis program was as follows: initial column temperature 100 °C, hold 2 min, ramp temperature to 280 °C at 15 °C/min, and hold for 5 min.

X-ray crystallographic determination

Single-crystal X-ray diffraction analyses of complexes **1**–**2** were performed on a Bruker Apex II CCD diffractometer operating at 50 kV and 30 mA using MoKα radiation ($\lambda = 0.71,073$ Å). Data collection and reduction were

Table 1 Crystallographic data for compounds **1–2**

Compound	**1**	**2**
Empirical formula	$C_{38}H_{40}Br_4N_2O_2Pd$	$C_{44}H_{56}Cl_2N_2Pd_2$
Formula weight	982.76	896.61
Temperature (K)	296 (2)	296 (2)
Crystal system	Triclinic	Monoclinic
Space group	P-1	$P2_1/n$
a (Å)	8.7889(10)	12.1647(7)
b (Å)	11.1925(12)	10.0977(6)
c (Å)	11.2702(12)	17.9704(10)
α (°)	62.534(2)	90.00
β (°)	82.656(2)	102.4890(10)
γ (°)	86.042(2)	90.00
V (Å^3)	975.55(18)	2,155.2(2)
Z	1	2
D (Mg m^3)	1.673	1.382
Limiting indices	$-10 \le h \le 10$, $-13 \le k \le 12$, $-13 \le l \le 11$	$-14 \le h \le 14$, $-12 \le k \le 9$, $-11 \le l \le 21$
Reflections collected/unique	10,260/3,465	12,139/3,850
R_{int}	0.0405	0.0229
F(000)	484	920
θ (°)	2.05–25.20	3.04–25.20
Goodness-of-fit on F^2	1.048	1.110
$R(I > 2\sigma)$	$R_1 = 0.0411$	$R_1 = 0.0216$
	$wR_2 = 0.0988$	$wR_2 = 0.0616$
R (all data)	$R_1 = 0.0659$	$R_1 = 0.0251$
	$wR_2 = 0.1117$	$wR_2 = 0.0642$
Largest diff. peak and hole (Å^{-3})	1.022, −0.970	0.309, −0.316

$R = \sum(||F_o| - |F_c||)/\sum|F_o|$

$wR = [\sum w(F_o^2 - F_c^2)^2/\sum w(F_o)^2]^{1/2}$

performed using the APEX II software [21]. Multiscan absorption corrections were applied for all the data sets using SADABS, as included in the APEX II program [21]. Small residual absorption effects were treated with XABS2 [22]. The structures were solved by direct methods and refined by least squares on F^2 using the SHELXTL program package [23]. All non-hydrogen atoms were refined with anisotropic displacement parameters. Hydrogen atoms attached to carbon and oxygen were placed in geometrically idealized positions and refined using a riding model. Crystallographic data are listed in Table 1. Selected bond lengths and angles are given in Table 2.

Results and discussion

To prepare complexes **1–2**, the Schiff base ligands were treated with Na_2PdCl_4 in equimolar amounts at room temperature in methanol. The reactions proceeded without reflux under mild conditions, thus preventing oxidation of Pd(II) to Pd(IV) [24].

Table 2 Selected bond lengths (Å) and angles (°)

Complex **1**			
Pd–O1^i	1.991(3)	Pd–N1^i	2.031(4)
O1^i–Pd1–O1	180	O1^i–Pd1–N1^i	92.05(14)
O1–Pd1–N1^i	87.95(14)	N1^i–Pd1–N1	180
Complex **2**			
Pd1–C2	1.979(2)	Pd1–Cl1	2.3271(6)
Pd1–Cl1^i	2.4538(6)	Pd1–N1	2.0344(17)
C2–Pd1–N1	81.40(8)	C2–Pd1–Cl1	94.83(6)
N1–Pd1–Cl1	176.08(5)	C2–Pd1–Cl1^i	177.62(7)
N1–Pd1–Cl1^i	97.17(5)	Cl1–Pd1–Cl1^i	86.569(19)

Symmetry codes: for **1** $i = 1 - x, -y, -z$; for **2** $i = 1 - x, 1 - y, -z$

The structure of complex **1** is shown in Fig. 1. The molecule structure is *trans*-[Pd(L1)$_2$], and the palladium atom lies on a crystallographic inversion center and assumes a square planar configuration. The Pd–O and Pd–N distances of 1.991(2) and 2.031(4) Å, respectively, are similar to those seen in related complexes [4, 25]. For instance, distances of 1.966(8) and 2.067(10) Å for the

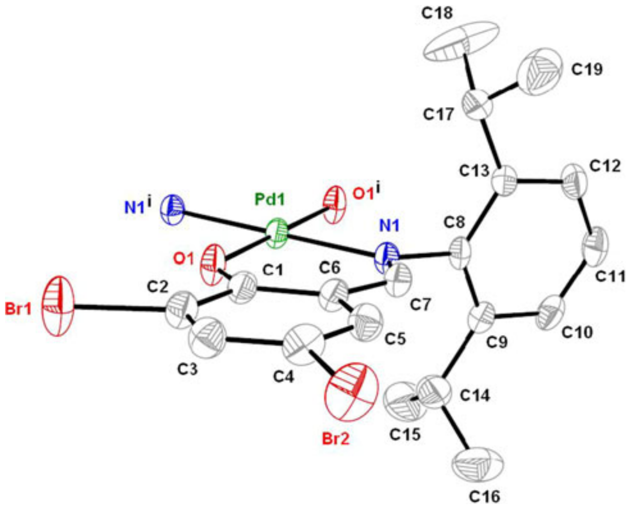

Fig. 1 The molecular structure of compound **1** with numbering scheme. All H atoms were omitted for clarity. Symmetry code: (*i*) $1 - x, -y, -z$

Pd–O and Pd–N bonds are found in a related bis(salicylideneaminato) palladium complex derived from 2-hydroxy-4-(*n*-hexyloxy)benzaldehyde and 4-*n*-hexylaniline [26]. The planes of the two phenyl rings are inclined by 3.98(2) and 88.31(4)°to the PdN_2O_2 coordination plane, respectively. In the six-membered chelate rings, the six atoms (Pd1, O1, C1, C6, C7, and N1) are essentially planar. The bite angle [N1–Pd1–O1 $=$ 92.04(2)°] is in good agreement with those found in a structurally related mononuclear complex [5, 27].

The molecular structure of complex **2** is shown in Fig. 2. Selected bond distances and angles are given in Table 2. In this complex, each Schiff base ligand (**L2**) is bonded to the di-μ-chloro-bridged unit through nitrogen atoms and an aromatic carbon atom, providing two equivalent five-membered N–C–Pd–C-chelate rings. The geometry at the Pd(II) center in **2** is square planar, with the two cyclometalated ligands in *a trans* arrangement with respect to the Pd···Pd axis. The Pd1–C2 bond [1.979(3) Å] is shorter than the expected value of 2.08 Å based on the sum of the covalent radii of carbon and palladium, but consistent with those found for related complexes where partial multiple-bond character of the Pd–C was assumed [28, 29]. The Pd1–N1 bond distance [2.034(2) Å] is in agreement with the sum of covalent radii for nitrogen and palladium [30], and similar to values reported earlier [28, 29]. The lengths of the Pd–Cl bond *trans* to C [2.454(2) Å] and the Pd–Cl bonds *trans* to N [2.327(5) Å] reflect the different *trans* influences exerted by the phenyl carbon and nitrogen atoms. In the five-membered chelate rings, the five atoms (Pd1, N1, C7, C1, and C2) are essentially planar. The bite angle [C2–Pd1–N1 $=$ 81.40(6)°] is in good agreement with those found in a structurally related μ-Cl dimer [29].

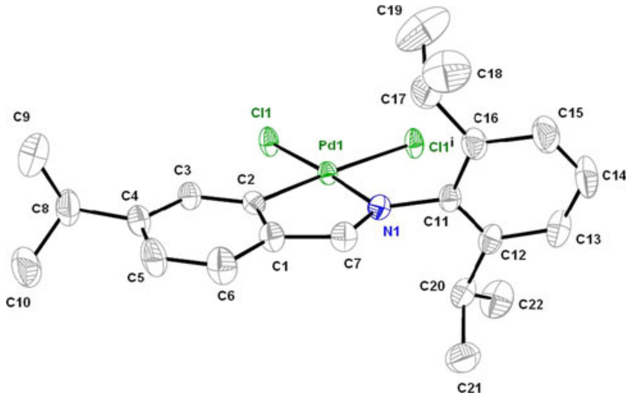

Fig. 2 The molecular structure of compound **2** with numbering scheme. All H atoms were omitted for clarity. Symmetry code: (*i*) $1 - x, -y, -z$

Powder X-ray diffraction analysis

In order to check the purity of complexes **1**–**2**, bulk samples were measured by X-ray powder diffraction at room temperature. As shown in Fig. 3, the peak positions of the experimental patterns are in a good agreement with the simulated patterns, which clearly indicates the high purity of the complexes.

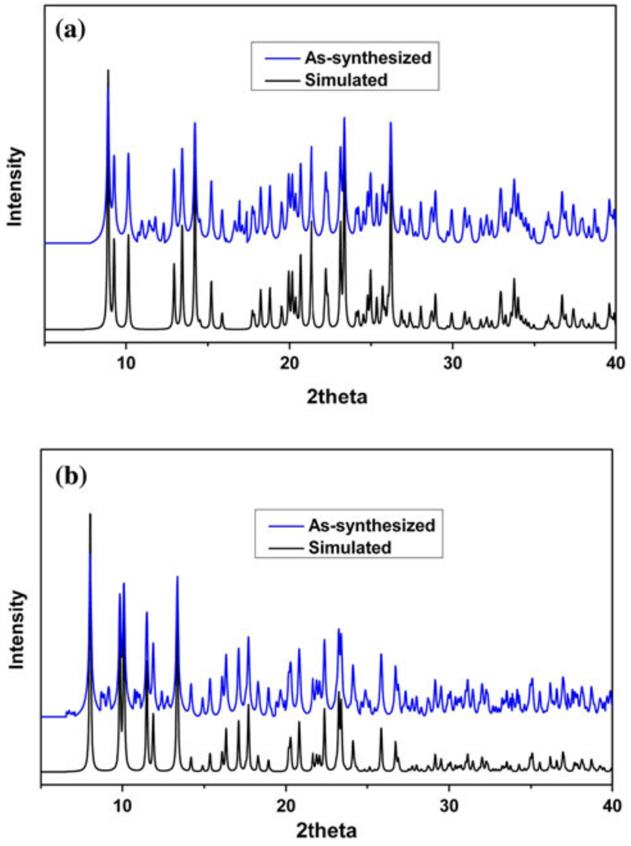

Fig. 3 PXRD patterns in complexes **1**–**2**, **a** for **1** and **b** for **2**

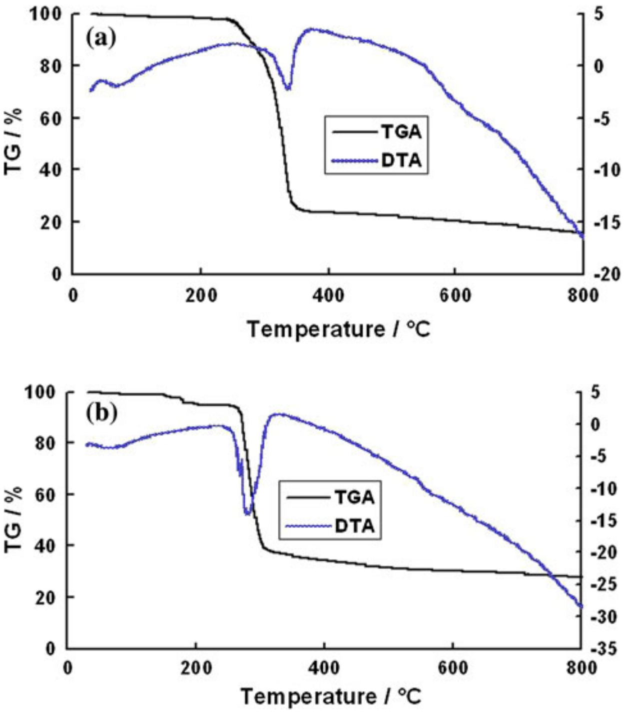

Fig. 4 Thermogravimetric curves (DTA and TG) for complexes **1** (**a**) and **2** (**b**)

IR spectra analysis

FT-IR spectra of ligands **HL1, L2, 1** and **2** were recorded as KBr pellets (Fig. S1–S2). In the IR spectrum, strong, broad bands at 3,473 cm^{-1} for **HL1**, 3,456 cm^{-1} for **L2**, 3,450 cm^{-1} for **1** and 3,467 cm^{-1} for **2** may be assigned to the *v*(O–H) stretching vibrations of water molecules (impurity). Features at 2,962, 2,883, and 1,622 cm^{-1} for **HL1**, 2,966, 2,871, and 1,641 cm^{-1} for **L2**, 2,962, 2,931, 2,875, and 1,608 cm^{-1} for **1**, 2,962, 2,871, and 1,597 cm^{-1} for **2** are associated with the methyl, methylene, and –CH=N– groups, respectively. The absorption peaks of the –CH=N– group in **1** and **2** are obviously blue-shifted against the related ligands, perhaps due to the conjugative effect between Pd^{2+} ions and the ligands.

Thermogravimetric analyses of complexes 1–2

The TG and DTA curves of **1** and **2** are shown in Fig. 4. Complex **1** has thermal stability as no clean weight-loss step occurs below 250 °C. The weight-loss step above 250 °C corresponds to decomposition of the structure. Complex **2** shows a weight loss of 8.2 % (150–200 °C), corresponding to the escape of two chlorine atoms (Calcd 7.9 %). Then, a sharp weight loss occurs above 250 °C due to decomposition of the structure.

Electronic absorption and emission properties of complexes 1–2

The UV–visible absorption spectra of **1** and **2** depicted in this work have been obtained. The UV–vis spectral data in DMF are listed in Table 3, and the absorption spectra are shown in Fig. 5. The intense absorptions at $\lambda_{max} = 279$ nm for **1**, $\lambda_{max} = 253$, 273 nm for **2** ($\varepsilon = \sim 10^4$ dm^3 mol^{-1} cm^{-1}) are assigned to intraligand transitions of the cyclometalated ligand. The ε value at 361 for **1** and 345 for **2** is 4,800 and 4,200 dm^3 mol^{-1} cm^{-1}, respectively, and we tentatively assign this band to a spin-allowed 4d(Pd) → π*(L^1) (^{1}MLCT) transition [2]. Absorption bands at $\lambda_{max} = 340$–400 nm in the related complexes $[Pd(C,N)_2]$ (HC,N = 2-phenylpyridine, 2-(2′-thienyl)pyridine, 7,8-benzoquinoline) have also been ascribed to MLCT

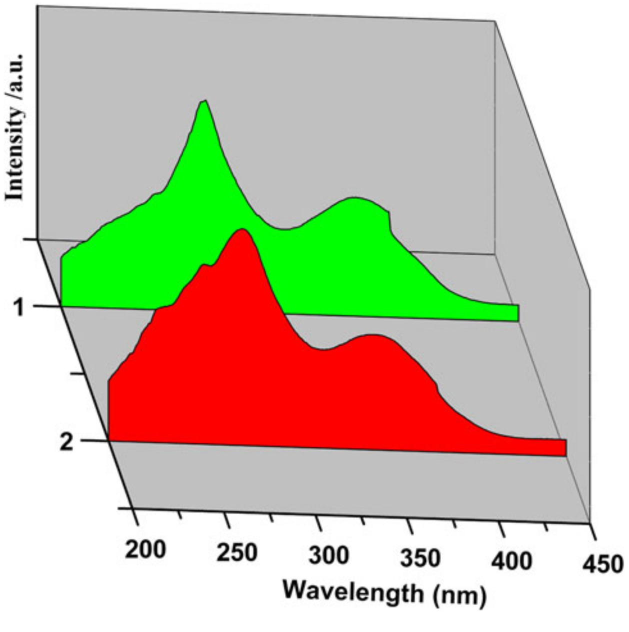

Fig. 5 UV–vis absorption spectra of **1** and **2** in DMF at 298 K

Table 3 Photophysical data

Compounds	Medium (T/K)	λ/nm (*e*/dm^3 mol^{-1} cm^{-1})	Emission λ/nm
1	DMF (298)	279 (34,200), 361 (4,800)	Non-emission
	Solid (298)	Non-tested	512, 644, 695, 716, 768
2	DMF (298)	253 (sh, 36,200), (273 (22,700), 345 (4,200)	non-emission
	Solid (298)	Non-tested	525, 570, 622, 690, 714, 765

transitions [31]. Ligand-field d–d transitions have been invoked for absorptions in the 340–400 nm range for ortho-metalated azobenzene Pd(II) complexes [32], but unreasonably high ε values (ca. 8 × 10^3 dm^3 mol^{-1} cm^{-1}) are reported. We reason that the ε values at 361 nm for **1** and 345 nm for **2** are also larger than would be expected for d–d transitions in Pd(II) derivatives.

As part of a continuing program dedicated to luminescent d^8 systems, the spectroscopic behavior of complexes **1**–**2** is presented. Both structures are non-emissive in DMF at room temperature, which is similar to previous reports [2, 3]. Solid-state emission luminescence spectra of **1**–**2** at room temperature are shown in Fig. 6. For **1**, the emission spectrum shows a shoulder at $\lambda_{max} = 512$ nm and four structureless bands at $\lambda_{max} = 644$, 695, 716, and 768 nm, respectively. For **2**, the emission spectrum shows two sharp bands at $\lambda_{max} = 525$, 570 nm, and four structureless bands at $\lambda_{max} = 622$, 690, 714, and 765 nm, respectively. Both the absorption and solid-state excitation spectra for **1**–**2** reveal the presence of low-energy ligand-field states in the 330–400 nm spectral region. The high-energy structures of **1** and **2** are assigned to a ^{3}IL excited state [2]. The broad structureless emission in the range of 600–800 nm is tentatively assigned to an excimeric ^{3}IL transition [2]. The luminescent lifetimes of solid **1** and **2** using an Edinburgh FLS S920 phosphorimeter with a 450-W xenon lamp as excitation source show lifetimes for **1** of $\tau_1 = 87.20$ ns, $\tau_2 = 190.45$ nm, and $\tau_3 = 1{,}805.10$ nm at 616 nm, for **2** of $\tau_1 = 69.92$ ns, $\tau_2 = 136.40$ nm, $\tau_3 = 1{,}714.26$ nm at 570 nm (Fig. 7).

Suzuki reaction catalysis

The results reveal that the base and solvent for the Suzuki reaction greatly influence catalytic activity (Table 4). The reaction temperature has less effect on the catalytic activity. Toluene is the best solvent for this catalytic system. In other organic solvents, for example, ethanol/water, ethylene glycol or DMF, relatively low yields of coupling products were obtained. Among five different bases investigated for these reactions, K_2CO_3 was found to be the most effective (Table 4, entry 1); Na_2CO_3, CH_3ONa, NaOAc, and NaOH were substantially less effective. KF failed to promote the reaction (Table 4, entry 10). Compared with other Pd(II) complexes containing Schiff bases, the catalytic activities of the present complexes for the Suzuki reaction proved to be highly effective [14].

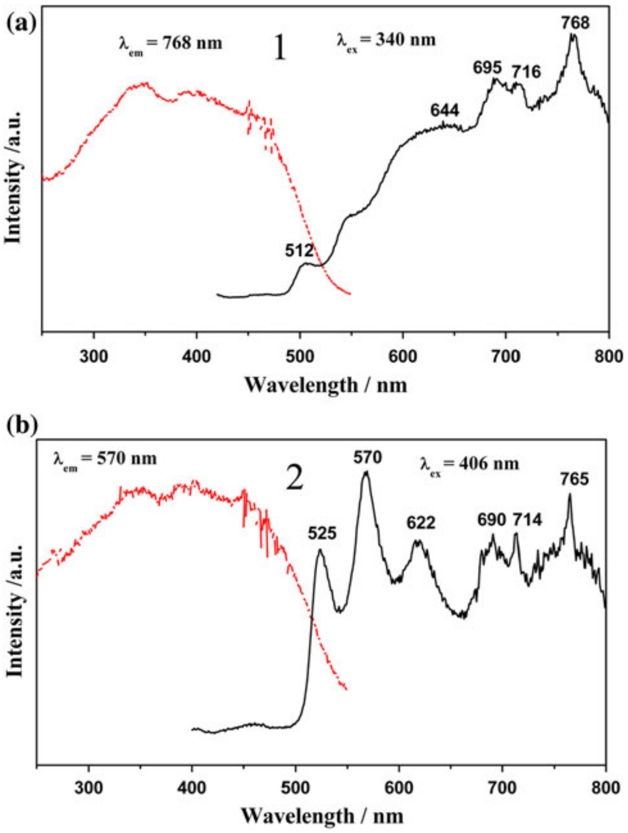

Fig. 6 Solid-state excitation and emission spectra of **a** **1** and **b** **2** at 298 K

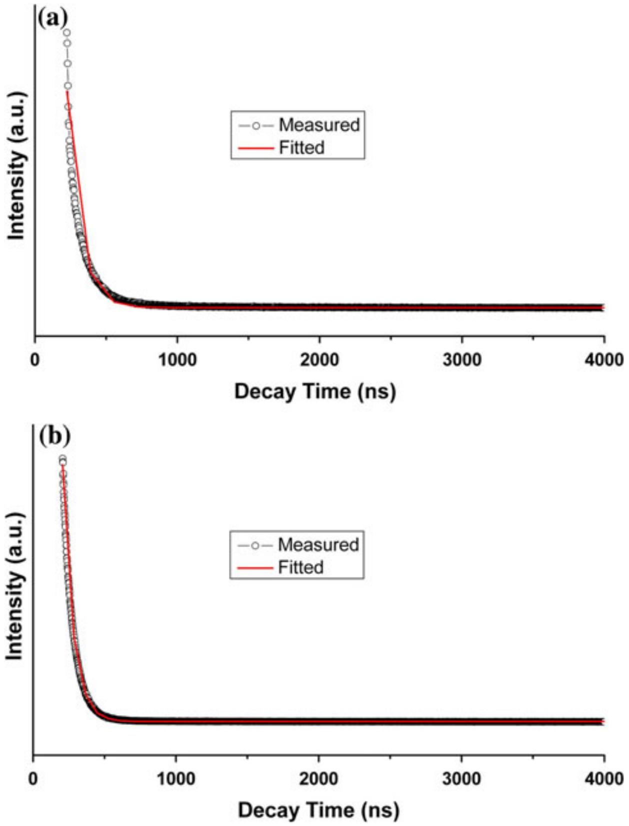

Fig. 7 Luminescent lifetimes of **a** **1** and **b** **2** in the solid state at 298 K

Table 4 The effect of base and solvent on the complexes **1**–**2** catalyzed Suzuki reaction of 4-bromotoluene with phenylboronic acid

Entry	Base	Solvent	Temp.(°C)	Atm.	Time (min)	Yields (%) **1/2**
1	K_2CO_3	Toluene	80	Air	50	92/95
2	K_2CO_3	Toluene	25	Air	50	78/80
3	K_2CO_3	Ethanol/water = 2:2	80	Air	50	73/76
4	K_2CO_3	Ethylene glycol	80	Air	50	76/77
5	K_2CO_3	DMF	100	Air	50	65/69
6	Na_2CO_3	Toluene	80	Air	50	56/59
7	CH_3ONa	Toluene	80	Air	50	51/53
8	NaOH	Toluene	80	Air	50	40/44
9	NaOAc	Toluene	80	Air	50	Trace
10	KF	Toluene	80	Air	50	–/–

Conclusion

In summary, we have described in this paper that the synthesis of two new Schiff base ligands and their Pd(II) complexes. Both **1** and **2** show good thermal stability and exhibit photoluminescence in the solid state at room temperature ($\tau_1 = 86.40$ ns, $\tau_2 = 196.21$ ns, $\tau_3 = 1{,}923.31$ ns at 768 nm for **1**, $\tau_1 = 69.92$ ns, $\tau_2 = 136.40$ ns, $\tau_3 = 1{,}714.26$ ns at 570 nm for **2**). Moreover, complexes **1** and **2** exhibit highly catalytic activities in the Suzuki coupling reaction of 4-bromotoluene with phenylboronic acid, which are also very sensitive to the choice of base and solvent.

Supporting information available

Fig. S1–S2 including the FT-IR spectrum of the ligands (**HL1** and **L2**) and the complexes **1**–**2.** Crystallographic data for the structures reported in this article have been deposited with the Cambridge Crystallographic Data Centre, CCDC 910681-910682 for **1** and **2**. Copies of this information may be obtained free of charge from the Director, CCDC, 12 Union Road, Cambridge, CB21EZ, UK (fax: +44 1223 336 033; e-mail: deposit@ccdc.cam.ac.uk or (http://www.ccdc.cam.ac.uk) or also available from the author on request.

Acknowledgments We are thankful for financial support of this work provided by Science and Technology Planning Project of Zhaoqing City (2012G030), Science and Technology Innovation Planning Project of Zhaoqing City (2012G013), and Distinguished Young Talents in Higher Education of Guangdong Province (2012LYM_0134).

References

1. Kumar S, Niranjan MS, Chaluvaraju KC, Jamakhandi CM, Kadaderar DJ (2010) J Curr Pharm Res 01:39
2. Lai SW, Cheung TC, Chan MCW, Cheung KK, Peng SM, Che CM (2000) Inorg Chem 39:255
3. Tzeng BC, Chan SC, Chan MCW, Che CM, Cheung KK, Peng SM (2001) Inorg Chem 40:6699
4. Zhang H, Norman DW, Wentzell TM, Irving AM, Edwards JP, Wheaton SL, Vogels CM, Westcott SA (2005) Transit Met Chem 30:63
5. Cariati F, Caruso U, Centore R, De Maria A, Fusco M, Panunzi B, Roviello A, Tuzi A (2004) Inorg Chim Acta 357:548
6. Centore R, Fort A, Panunzi B, Roviello A, Tuzi A (2004) Inorg Chim Acta 357:913
7. Cummings SD, Eisenberg R (1996) J Am Chem Soc 118:1949
8. Wong KH, Chan MCW, Che CM (1999) Chem Eur J 5:2845
9. Neve F, Crispini A, Di Pietro C, Campagna S (2002) Organometallics 21:3511
10. Crosby GR (1975) Acc Chem Res 8:231
11. Miyaura N, Suzuki A (1995) Chem Rev 95:2457
12. Suzuki A (1999) J Organomet Chem 576:147
13. Polshettiwar V, Len C, Fihri A (2009) Coord Chem Rev 253:2599
14. Isiam SM, Mondal P, Tuhina K, Roy AS, Mondal S, Hossain D (2010) 20:264
15. Kim JW, Kim JH, Lee DH, Lee YS (2006) Tetrahedron Lett 47:4745
16. Mukherjee S, Samanta S, Roy BC, Bhaumik A (2006) Appl Catal A Gen 301:79
17. Shimizu K, Koizumi S, Hatamachi T, Yoshida H, Komai S, Kodama T, Kitayama Y (2004) J Catal 228:141
18. Bulut H, Artoka L, Yilmaz S (2003) Tetrhedron Lett 44:289
19. Guo HF, Pan Y, Ma DY, Lu K, Qin L (2012) Transition Met Chem 37:661
20. Fukuda H, Amimoto K, Koyama H, Kawato T (2003) Org Biomol Chem 1:1578
21. Bruker D (2004) APEXII software, version 6.3.1. Bruker AXS Inc, Madison
22. Parkin S, Moezzi B, Hope H (1995) J Appl Cryst 28:53
23. Sheldrick GM (2008) Acta Cryst A64:112
24. Naeimi H, Moradian M (2010) J Coord Chem 63:156
25. Zhu L, Bakhtiar R, Kostic NM (1998) J Biol Inorg Chem 3:383
26. Day VW, Glick MD, Hoard JL (1968) J Am Chem Soc 90:4803
27. Lanfredi AMM, Ugozzoli F (1985) Acta Cryst C41:192
28. Crispini A, Munno GD, Ghedini M, Neve F (1999) J Organmet Chem 427:409
29. Fuchita Y, Yoshinaga K, Hanaki T, Kawano H (1999) Kinoshita Nagaoka J 580:273
30. Pauling L (1960) The nature of chemical bond. Cornell University Press, New York
31. Maestri M, Sandrini D, Balzani V, Von Zelewsky A, Jolliet P (1988) Helv Chim Acta 71:134
32. Wakatsuki Y, Yamazaki H, Grutsch PA, Santhanam M, Kutal C (1985) J Am Chem Soc 107:8153